

Anisotropic superconductivity in C_4KHg

A. Chaiken* and M.S. Dresselhaus

*Department of Physics, Massachusetts Institute of Technology, Cambridge,
Massachusetts 02139*

T.P. Orlando

*Department of Electrical Engineering and Computer Science,
Massachusetts Institute of Technology, Cambridge, Massachusetts 02139*

G. Dresselhaus and P.M. Tedrow

*Francis Bitter National Magnet Laboratory, Massachusetts Institute of
Technology, Cambridge, Massachusetts 02139*

D.A. Neumann

*National Institute of Science and Technology,
Gaithersburg, Maryland 20899*

W.A. Kamitakahara†

Department of Energy, Washington, D.C. 20545

(Received 15 May 1989)

Superconducting transition temperatures between 0.7 and 1.5 K are reported for the stage-1 potassium-mercury graphite intercalation compound (GIC) C_4KHg . A number of experiments have been performed to investigate the differences between the C_4KHg samples at either extreme in T_c . The only structural difference appears to be that the β phase (characterized by a c -axis lattice constant $I_c=10.83 \text{ \AA}$) is consistently found in the lower- T_c samples, while the higher- T_c samples always contain only the α phase ($I_c=10.24 \text{ \AA}$). Adding a minute amount of hydrogen to the $T_c=0.8 \text{ K}$ samples raises their transition temperature to 1.5 K. Measurements of the angular dependence of the critical field suggest that the higher- T_c samples have type-I character for a range of applied field orientations near $\mathbf{H} \parallel \hat{c}$. The temperature dependence of the upper critical field of C_4KHg shows extended linearity of $H_{c2,\perp\hat{c}}(T)$ for both types of samples. The critical-field data of C_4KHg and other GIC's are discussed in light of multiband and anisotropic Fermi-surface models of superconductivity. The thermodynamic parameters obtained from the critical-field experiments are compared to the specific-heat data of Alexander *et al.* A charge-density-wave hypothesis first proposed by DeLong and Eklund is suggested to explain the hydrogen-induced enhancement of T_c .

I. INTRODUCTION

The superconducting graphite intercalation compounds (GIC's) are among the most intensively studied layered superconductors.^{1,2} Initially most research efforts centered on the first-stage compounds C_8M , where M is a heavy alkali metal.^{3,4} These compounds consist of alternate graphene (hexagonal carbon network) planes and layers of alkali-metal atoms. The occurrence of superconductivity in these GIC's is surprising, since neither of the starting constituents (graphite or the alkali metal) is superconducting.³ In recent years the focus of GIC superconductivity research has shifted to the ternary compounds⁵ in which the intercalant unit is made up of an alkali metal and a heavy metal in a trilayer sandwich.

An extensive study of superconductivity in the MHg GIC's and MTl GIC's was performed by Iye and Tanuma.⁶ Superconductivity of the second-stage compound C_8KHg was also studied by Pendryns *et al.*⁷ Sev-

eral unusual features were found:⁶⁻⁸ an unusual temperature dependence of the upper critical-field $H_{c2}(T)$, and critical-field anisotropy ($H_{c2,\perp\hat{c}}/H_{c2,\parallel\hat{c}}$) ratios as large as 47. The unusual temperature dependence consisted of either extended linearity of $H_{c2}(T)$ [i.e., $H_{c2}(T) \propto (1 - T/T_c)$, to unusually low temperatures] or positive curvature ($d^2H_{c2}/dT^2 > 0$) of $H_{c2}(T)$. Positive curvature of $H_{c2}(T)$ is contrary to the usual low-temperature saturation of $H_{c2}(T)$ seen in most type-II superconductors.^{9,10} Yet positive curvature or extended linearity of $H_{c2}(T)$ appears to be a common feature of nearly all layered superconductors.¹¹ An understanding of this anomalous critical-field behavior is particularly of interest because the high- T_c oxide superconductors are also anisotropic layered materials.

The superconducting transition temperature of C_4KHg has been reported to be anywhere in the range from 0.7 to 1.5 K.^{6,12,13} Understanding this T_c variation may well be an important first step in determining the stage depen-

dence of T_c in the KHg GIC's. Raman scattering¹² and transmission electron microscopy¹⁴ (TEM) have been employed by Timp *et al.* to examine the differences between C_4KHg samples at the two extremes of T_c , but no full comparison of the superconducting properties has been made. In this work a detailed study of the superconductivity of C_4KHg is reported, including neutron-diffraction, critical-field, and hydrogenation experiments. Preliminary results have been reported previously.^{13,15}

II. SAMPLE PREPARATION AND CHARACTERIZATION

The C_4KHg specimens used in these studies were synthesized using the two-zone vapor-phase intercalation technique pioneered for these materials by El Makrini *et al.*^{16,17} The starting amalgams ranged in composition from K_2Hg_3 to K_5Hg_4 . No systematic effects were seen as a function of the starting alloy composition. The amalgam temperature during intercalation was varied between 200 and 260 °C. In addition, the graphite temperature was independently varied from 0 to 10 °C above the amalgam temperature. The intercalation reaction was always allowed to proceed for at least two weeks. The intercalation ampoules were withdrawn from the furnace after they had cooled nearly to room temperature.

Timp found that the application of a 10 °C temperature difference between the graphite and the amalgam during intercalation increased the disorder in the intercalant layers and lowered T_c .¹² He reported a gold color for lower- T_c disordered specimens and a pink color for ordered $T_c = 1.5$ K ones.¹² Timp also reported that a temperature difference between the graphite and the amalgam increases the amount of the $(\sqrt{3} \times 2)R(30^\circ, 0^\circ)$ phase as compared with the majority $(2 \times 2)R0^\circ$ phase.¹² The $(2 \times 2)R0^\circ$ in-plane ordering is associated with a 10.24-Å c -axis lattice constant and has been called the α phase.¹⁸ The $(\sqrt{3} \times 2)R(30^\circ, 0^\circ)$ ordering has been positively identified with the c -axis lattice constant $I_c = 10.83$ Å by Kamitakahara *et al.*¹⁹ The $I_c = 10.83$ Å phase is called the β phase.²⁰ Kim *et al.*²¹ report that application of a temperature difference during intercalation increases the amount of the β phase, in agreement with the finding of Timp.¹²

In this study, x-ray and neutron diffraction were used to characterize the C_4KHg specimens for staging fidelity and phase purity. The x-ray characterization was performed at MIT using Mo $K\alpha$ radiation in a θ - 2θ geometry. Neutron-diffraction ($00l$) spectra were taken at the National Institute of Science and Technology research reactor using the BT-4 triple-axis neutron diffractometer with thermal neutrons of wavelength 1.528 Å. Neutron-diffraction spectra of pink (single-phase) and gold (mixed-phase) C_4KHg specimens are shown in Fig. 1. Interestingly, neutron diffraction revealed the presence of about 10% β phase in a sample which showed only α -phase peaks in x-ray diffraction spectra. This inconsistency is undoubtedly due to the limited penetration

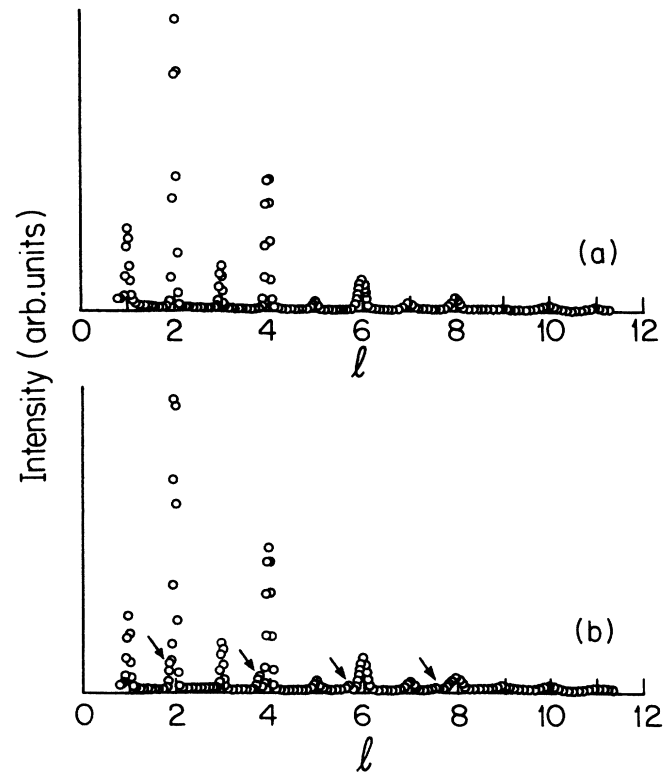


FIG. 1. Neutron diffraction ($00l$) spectra of pink and gold C_4KHg specimens. (a) Only the peaks of the $I_c=10.24$ Å α phase are visible in the pink specimen. (b) Both the $I_c=10.24$ Å α phase and the $I_c=10.83$ Å β phase show peaks in the gold specimen. The β -phase peaks are marked with arrows.

depth of x rays in C_4KHg (about 35 μm).²² Obviously caution is advisable when using x-ray diffraction to interpret the results of experiments that measure the bulk properties of C_4KHg .

In all, over 20 batches of C_4KHg were prepared and characterized. The assertion that a 5–10 °C temperature difference increases the amount of the β phase was strongly confirmed. However, the β phase can also be formed under nominally isothermal intercalation conditions, sometimes even in the same ampoule with pure α -phase specimens. It seems likely that variables that are difficult to control precisely (such as the condition of the edges of the graphite flake) may affect the speed of the intercalation reaction and determine the final ratio of the two phases in a sample. Pure β -phase specimens have never been produced, as previously noted by Lagrange.²³ Pure α -phase specimens were routinely produced and found to be pink in color, while mixed ($\alpha + \beta$)-phase specimens were variously gold or copper in color.

In order to derive quantitative structural information from the neutron diffraction data shown in Fig. 1, the integrated intensities of the diffraction patterns were fit to a five-layer model²⁴ of the unit cell. A gradient-least-squares optimization algorithm²⁵ was employed to obtain the residual-minimizing parameters.²⁶ The Lorentz factor was corrected for the specimen's mosaic spread using a standard procedure.²⁷ Further details of the analysis

TABLE I. Parameters obtained from fits to C_4KHg neutron and x-ray diffraction data. I_c is the c -axis lattice constant, N_{Hg} is the number of Hg atoms per four carbon atoms, z_K is the distance between the potassium layers and the center of the intercalant sandwich, and Δz is the separation of the Hg layers. The majority and minority phases have also been called the α and β phases, respectively.

Spectrum type	I_c (Å)	N_{Hg}	z_K (Å)	Δz (Å)
Gold, majority (α)	10.24	1.1	2.0	0.18
Pink, majority (α)	10.24	1.0	2.3	0.0
Majority (α) ^{a,b}	10.24	1.0	2.1	0.0
Minority (β) ^{a,b}	10.83	1.3	2.8	0.0
Majority (α) ^c	10.16	1.0	2.34	0.25

^aReference 29.

^bReference 30.

^cReference 18.

are given in Ref. 28. Only the majority α -phase intensities were fit because the number of observed β -phase peaks was too small. The results of the analysis are compared to the parameters obtained by previous investigators in Table I.

Careful examination of Table I shows that the structural and stoichiometric differences between the majority (α) phases of the gold and pink specimens are small. The parameters in Table I obtained from the structure-factor fits are in good agreement with those of Ref. 29. In conjunction with the results of wet chemical analysis on samples whose T_c was known,²⁸ the results in Table I contradict the assertion^{13,31} that the gold mixed-phase C_4KHg samples are mercury deficient. The general conclusion from the neutron diffraction experiments is that the majority-phase material in the gold and pink samples appears to be the same. The only reproducibly observed difference in the normal-state properties of the gold and pink C_4KHg samples is that the gold ($T_c = 0.8$ K) samples are mixed phase, while the pink ($T_c = 1.5$ K) samples are pure α phase. The superconducting properties of the single-phase and mixed-phase samples are compared in detail below.

III. EXPERIMENTAL DETAILS

The angular and temperature dependence of the upper critical field H_{c2} of C_4KHg were previously measured by Iye and Tanuma⁶ for samples with a zero-field transition temperature of about 0.8 K. The new study reported here has two goals. One goal is to determine if the superconducting properties of the gold mixed-phase C_4KHg samples are similar to those previously reported.⁶ The other aim is to measure the critical fields of the pink single-phase C_4KHg specimens to see what can be learned about their differences relative to the gold mixed-phase samples.

After characterization for staging and phase purity, the GIC samples were affixed to copper mounts using Apiezon N grease. These mounts were designed so that the samples could not move during the H_{c2} measure-

ments. The sample holders were fixed inside Pyrex tubes, which were then filled with purified helium gas to ensure good thermal contact with the bath at cryogenic temperatures. After mounting, the (00 l) x-ray spectrum of the sample was taken again to ensure that no sample deterioration had occurred.

The superconducting transitions were measured by monitoring the ac susceptibility of the sample as the temperature or magnetic field was swept. A standard ac inductance bridge³² with excitation field 0.2 Oe at 490 Hz was used to monitor the magnetic susceptibility. Temperature readings were obtained from a calibrated germanium resistor (Lake Shore GR-200A-100), and from a capacitive pressure sensor (MKS Instruments, Inc., Baratron) that monitored the 3He vapor pressure. Given the accuracy with which the induced signal and dimensions of the intercalated specimen are known, it can be stated that the superconducting areal fraction of the GIC's used in this experiment was typically $(80 \pm 20)\%$. The zero-field transition temperature, T_c , was defined to be the intersection of a line drawn tangent to the most linear part of the inductance versus temperature points with the temperature-independent upper part of the transition at a point where the sample was 90% normal (see inset of Fig. 2). The transition width, ΔT_c , was defined as the interval between the 10% and 90% completion temperatures of the transition. The dimensionless (T_c -independent) figure of merit used here to characterize sample quality is $\Delta T_c/T_c$. Values of $\Delta T_c/T_c$ ranged from

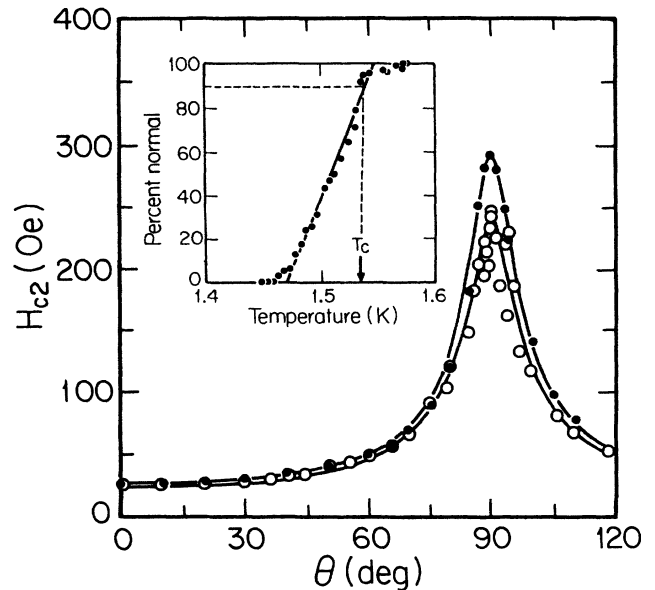


FIG. 2. Critical field H_{c2} as a function of the angle θ for lower- T_c C_4KHg samples. Fits (solid lines) were calculated using Eq. (1). Data are for a gold C_4KHg specimen with $T_c=0.95$ K (o) and also for a $T_c=0.73$ K sample (•) from Ref. 34. For the $T_c=0.95$ K sample, $1/\epsilon = 10.0$ and $H_{c2}(0^\circ)=24$ Oe with a residual $\mathcal{R}=0.29$. For data of Ref. 34, $1/\epsilon=11.3$, $H_{c2}(0^\circ)=26$ Oe, and $\mathcal{R}=0.090$. The inset shows how T_c was determined from the zero-field superconducting transition of one of the samples.

about 0.2 for poorly ordered samples to about 0.01 for well-ordered specimens.²⁸ H_{c2} is determined graphically from plots of inductance versus field and is defined as the field where a line drawn tangent to the most linear part of the normal-superconducting transition intersects the H -independent upper portion of the field sweep. (This is the same definition as was used in Ref. 6.) The angle θ that was varied in the angular dependence of the H_{c2} measurements is defined as the angle between the applied field and the crystallographic c axis. (Note that this angle is the complement of that usually called θ in the thin-film superconductivity literature.³³) The possible influence of flux-trapping and flux creep effects on the H_{c2} measurements was experimentally investigated and found to be unimportant for the samples used in this study.

IV. EXPERIMENTAL RESULTS

A. $H_{c2}(\theta)$ in C_4KHg

In Fig. 2, $H_{c2}(\theta)$ data are shown for two lower- T_c C_4KHg samples, one a gold $T_c = 0.95$ K specimen prepared at MIT, and the other a $T_c = 0.73$ K sample whose critical fields were reported by Iye and Tanuma.³⁴ The solid curves are fits to the formula

$$H_{c2}(\theta) = \frac{H_{c2}(0^\circ)}{(\cos^2 \theta + \epsilon^2 \sin^2 \theta)^{1/2}}, \quad (1)$$

where ϵ is the critical-field anisotropy parameter of Morris, Coleman, and Bhandari,³⁵ defined by

$$\epsilon \equiv H_{c2,\parallel\hat{c}}/H_{c2,\perp\hat{c}}, \quad (2)$$

and $H_{c2}(0^\circ)$ is $\hat{H}_{c2,\parallel\hat{c}}$. The fits were chosen to minimize the residual parameter²⁵ \mathcal{R} :

$$\mathcal{R} = \sum_i (H_i^{\text{expt}} - H_i^{\text{theor}})^2 / (\sigma_i^2 \nu), \quad (3)$$

where the errors σ_i are estimated as

$$\sigma_i(\theta) = 0.1 H_i^{\text{expt}} (1.0 + \sin \theta), \quad (4)$$

and ν is the number of free parameters. This form for $\sigma_i(\theta)$ accounts for the fact that a small error in reading θ produces a much larger error in H_{c2} when θ is near 90° than when θ is near 0° . Equation (1) describes the angular dependence of the critical field of anisotropic three-dimensional-coupled superconductors with uniaxial symmetry.^{35,36} As Fig. 2 shows, this formula gives a good description of the $H_{c2}(\theta)$ data for the lower- T_c gold C_4KHg samples.

The angular dependence of the upper critical-field $H_{c2}(\theta)$ data for two $T_c = 1.5$ K samples is shown in Fig. 3 along with two curves produced by Eq. (1). The curve marked by open circles (o) is the residual-minimizing curve according to the definition in Eq. (3). Using other reasonable functional forms for $\sigma_i(\theta)$ in Eq. (3) [such as assuming an angle-independent error $\sigma_i(\theta) = \sigma$] did not

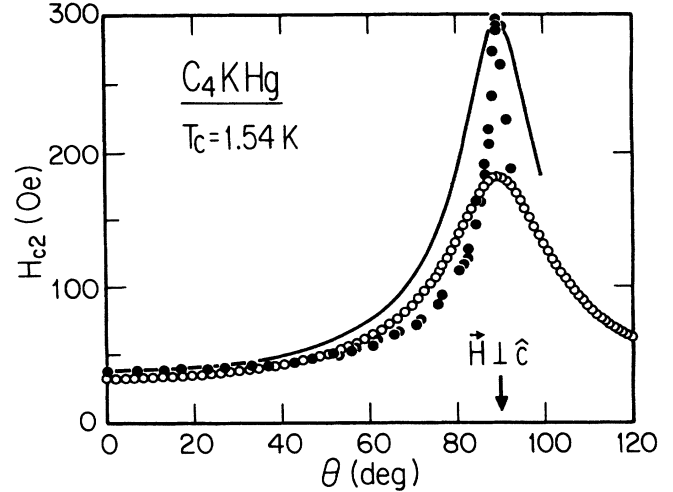


FIG. 3. Critical field H_{c2} as a function of the angle θ for a pink $T_c = 1.54$ K C_4KHg sample at $t \equiv T/T_c = 0.57$. Fits (solid line and o) were both calculated using Eq. (1). The curve marked with o is the residual-minimizing fit, which was produced with parameters $H_{c2}(0^\circ) = 33$ Oe and $1/\epsilon = 5.5$. For this fit, $\mathcal{R} = 1.25$. The solid curve is the result of forcing the fit through the data points at $\theta = 0^\circ$ and 90° . The resulting parameters are $H_{c2}(0^\circ) = 38.5$ Oe, $1/\epsilon = 7.7$, and $\mathcal{R} = 4.49$.

produce a fit that goes through the peak of the data. If the fit is forced through the data at $\theta = 90^\circ$, the solid curve in Fig. 3 is the result. Extensive experience in trying to fit the $H_{c2}(\theta)$ data of $T_c = 1.5$ K C_4KHg samples shows that Eq. (1) is inadequate as a detailed description of the experimental results. The role of sample quality on the functional form of $H_{c2}(\theta)$ was investigated in detail²⁸ and cannot explain the experimental deviations from Eq. (1). Possible causes for the poor fit quality, such as sample polycrystallinity and improper alignment, were studied in detail and found to be unimportant.²⁸

The specific-heat data of Alexander *et al.*³⁷ suggest an alternative explanation for the deviations in Fig. 3. Using the linear specific-heat coefficient $\gamma = 0.95$ mJ/mol K² measured by Alexander *et al.*, the zero-temperature thermodynamic critical field H_c can be estimated using the standard formula³³ $H_c(T = 0) = (2\pi\gamma T_c^2)^{1/2}$. No superconducting transition was measured down to 0.8 K during the specific-heat measurements,³⁷ so it is not clear that this linear specific-heat coefficient is appropriate for a $T_c = 1.5$ K sample. Nonetheless, an estimate of H_c can be made if one further assumes a $(2 \times 2)R0^\circ$ structure in order to calculate the molar volume. This procedure gives 112 Oe for H_c at $T = 0$ K for the $T_c = 1.5$ K pink samples, and 53 Oe for the $T_c = 0.8$ K gold samples. Using the usual quadratic form for the temperature dependence of H_c results in an estimate of 75 Oe for the thermodynamic critical field for the pink samples at the reduced temperature $t \equiv T/T_c = 0.57$. Since, as Fig. 3 shows, 75 Oe is larger than the measured $H_{c2}(\theta)$ for θ less than about 70° , this value of H_c suggests that superconductivity in $T_c = 1.5$ K C_4KHg samples is type I in character

for most applied field orientations.

When H_c is greater than H_{c2} , H_c will be measured as the upper critical field. Since H_c is a thermodynamic quantity, it is expected to be angle independent. If type-I superconductivity is present for some range of angles, one expects a modified angular dependence $\hat{H}_{c2}(\theta)$ defined by

$$\hat{H}_{c2}(\theta) \equiv \begin{cases} H_{c2}, & H_{c2}(\theta) > H_c \text{ (type-II region)} \\ H_c, & H_{c2}(\theta) < H_c \text{ (type-I region)}. \end{cases} \quad (5)$$

This piecewise continuous type of angular dependence has previously been observed^{4,38} in C₈K and in TaN. Using Eq. (1) for $H_{c2}(\theta)$, the $\hat{H}_{c2}(\theta)$ dependence defined by Eq. (5) has been fit to the angular-dependence data for the $T_c=1.5$ K C₄KHg samples. In the fits to Eq. (5), H_c was taken as a free parameter in addition to $H_{c2}(0^\circ)$ and ϵ . The resulting fit is shown in Fig. 4. Consultation of standard statistical tables²⁵ shows that the addition of the third free parameter H_c is justified by the factor of 1.5 reduction in the residual index. The hypothesis of type-I superconductivity in the higher- T_c pink C₄KHg specimens therefore appears to be justified not only by the specific-heat measurements of Alexander *et al.*,³⁷ but also by the improvement in the $H_{c2}(\theta)$ fits provided by the use of Eq. (5).

B. $H_{c2}(T)$ in C₄KHg

$H_{c2}(T)$ data for a $T_c=1.5$ K C₄KHg sample are shown in Figs. 5 and 6. The data were taken with the applied field both parallel (Fig. 5) and perpendicular (Fig. 6) to

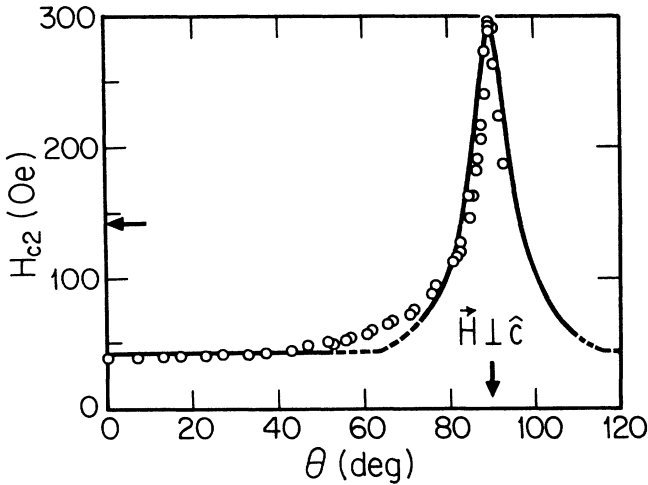


FIG. 4. $\hat{H}_{c2}(\theta)$ data for a $T_c=1.54$ K C₄KHg sample at $t=0.57$. Same data (o) as in Fig. 3, only now fit to the modified angular dependence of Eq. (5), which allows for type-I superconductivity near $\theta = 0^\circ$. Parameters for the fit are $\hat{H}_{c2}(0^\circ)=19$ Oe, $1/\epsilon=15.5$, and $H_c=43$ Oe, while $\mathcal{R}=0.84$. The remaining deviations in the wings of the peak may be attributable to angle-dependent demagnetization effects. The arrow on the left axis marks the estimated magnitude of $H_c=142$ Oe after correction for demagnetization (see text). This value of H_c would imply type-I behavior for $\theta < 80^\circ$, and type-II behavior for $\theta > 80^\circ$.

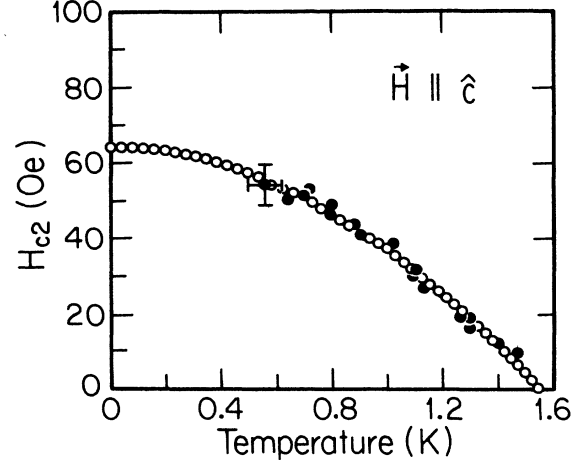


FIG. 5. Critical fields vs reduced temperature with $\vec{H} \parallel \hat{c}$ for a $T_c \approx 1.5$ K pink C₄KHg sample. Solid circles (●) denote data points; the open circles (o) denote a quadratic fit to the data with $H_{c2}(0) = 64.0$ Oe, $T_c=1.55$ K and $\mathcal{R}=1.2 \times 10^{-2}$.

the c axis of the graphene planes. In Fig. 5, the $H_{c2,\parallel\hat{c}}$ data are shown along with the best fit to the quadratic form

$$H_{c2,\parallel\hat{c}} = H_{c2,\parallel\hat{c}}(0)(1 - t^2).$$

This quadratic temperature dependence is expected for a type-I superconductor.

For the $H_{c2,\perp\hat{c}}$ data in Fig. 6, one of the fits is a simple straight line, while the other is calculated from the Werthamer-Helfand-Hohenberg (WHH) equation, which describes the temperature dependence of the upper critical field of a typical type-II superconductor.^{9,39} For the

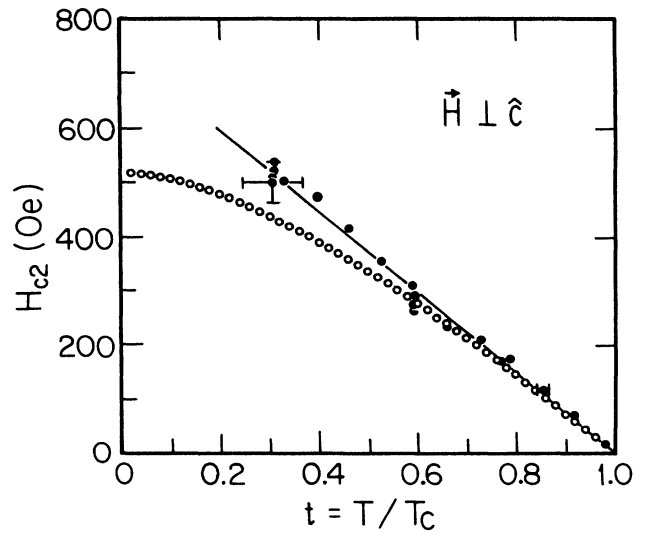


FIG. 6. Comparison of the WHH model and linear fits to the $H_{c2,\perp\hat{c}}(T)$ data taken on a pink $T_c=1.54$ K sample. (●) denote data points, the solid line denotes a linear fit with $H_{c2}(0)=748$ Oe, $T_c=1.52$ K, and $\mathcal{R}=0.69$. (o) denote WHH model fits with $H_{c2}(0)=518$ Oe, $T_c=1.53$ K, and $\mathcal{R}=1.6$.

$T_c=1.5$ K samples, the residuals for the linear fit are consistently at least a factor of 2 lower than those for the WHH fit. Thus we conclude that $H_{c2}(T)$ for the $T_c=1.5$ K pink C_4KHg samples exhibits extended linearity. The question of extended linearity cannot be decided for the lower- T_c mixed-phase samples because their data (not shown) extend over a smaller reduced temperature range due their lower T_c values.

The most convincing demonstration of the deviation of the $H_{c2,\perp\hat{c}}(T)$ data above the typical type-II superconductor curve is displayed in Fig. 7. By plotting the reduced field, $h^* \equiv \hat{H}_{c2}/(T_c d\hat{H}_{c2}/dT)$ versus reduced temperature ($t \equiv T/T_c$), all the $\hat{H}_{c2}(T)$ data for five different C_4KHg samples can be displayed together. $dH_{c2,\perp\hat{c}}/dT$ values obtained from linear fits range from about 500 Oe/K for the pink samples to about 800 Oe/K for the gold specimens of Iye and Tanuma.⁶ From the best linear fits to the $\hat{H}_{c2,\parallel\hat{c}}(T)$ data, the $d\hat{H}_{c2,\parallel\hat{c}}/dT$ values ranged from 60 Oe/K for the pink $T_c=1.5$ K samples to 75 Oe/K for the gold $T_c = 0.8$ K samples. The residual index for the linear fit to all the data in Fig. 7 is $\frac{3}{4}$ that of the WHH fit, indicative of about a 90% probability that the linear fit describes the data better.²⁵ Figure 7 also shows that at $t \approx 0.3$ (the lowest accessible reduced temperature) the data have already reached $h^* \approx 0.7$, which is the zero-temperature value of h^* calculated using the WHH formalism.⁹ Therefore, while it would be interesting to measure $H_{c2,\perp\hat{c}}(t)$ to lower reduced temperatures and see larger deviations from the WHH theory, the avail-

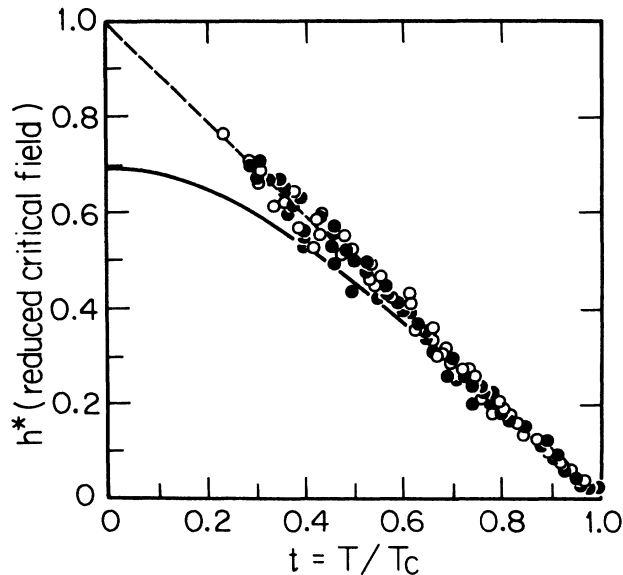


FIG. 7. Summary of $H_{c2}(t)$ experiments for five specimens with T_c between 1.5 and 0.7 K, including both $\hat{H}_{c2,\parallel\hat{c}}(\Delta)$ and $H_{c2,\perp\hat{c}}(0)(\Delta)$ data. The dimensionless quantities that are plotted are the reduced upper critical field (h^*) vs reduced temperature (t). The 143 data points were taken on five different GIC's. The solid curve is the best two-parameter WHH model fit to the data with $\mathcal{R}=1.7$. The dashed line is the best linear fit to the data with $\mathcal{R}=1.3$. Both fits have $dh^*/dt = -1$ at $t = 1$.

able data convincingly demonstrate a deviation from the WHH functional form.

If the critical field were linear for both field orientations, then the anisotropy parameter ϵ would be a constant, independent of temperature

$$\epsilon = \left(\frac{d\hat{H}_{c2,\parallel\hat{c}}/dT}{dH_{c2,\perp\hat{c}}/dT} \right). \quad (6)$$

Equations (1) and (2) together define ϵ . Within the context of the anisotropic Ginzburg-Landau model, Eq. (6) should be equivalent to the definition for ϵ . The values of ϵ obtained from the $H_{c2}(\theta)$ fits using the definition [Eq. (2)] will agree with those obtained from $H_{c2}(T)$ fits using Eq. (6) only if type-I superconductivity is not present. The equivalence of the two definitions of ϵ is therefore a test of the quantitative applicability of the anisotropic Ginzburg-Landau model. Clearly Eqs. (2) and (6) cannot be consistent if ϵ as obtained from the $H_{c2}(\theta)$ fits is even slightly temperature dependent.

A graphical test of the constancy of ϵ is as follows. If ϵ is temperature independent, the only temperature-dependent quantity in Eq. (1) should be $H_{c2}(0^\circ)$. Therefore plots of $H_{c2}(\theta)/H_{c2}(0^\circ)$ versus θ should lie directly on top of one another, since all the temperature dependence has presumably been removed. A plot of $H_{c2}(\theta)/H_{c2}(0^\circ)$ is shown in Fig. 8 for a $T_c=1.5$ K C_4KHg

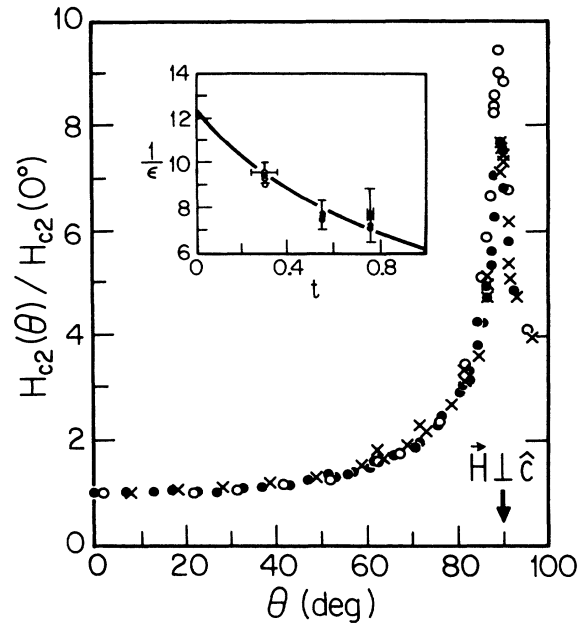


FIG. 8. Demonstration of temperature-dependent anisotropy parameter ϵ in C_4KHg . $1/\epsilon$ is $H_{c2}(90^\circ)/H_{c2}(0^\circ)$. Data are for a $T_c=1.54$ K pink C_4KHg sample, at the following reduced temperatures. (o), $t=0.29$; (\bullet), $t=0.55$; (\times), $t=0.76$. All $H_{c2}(0^\circ)$ values were determined from the experimental data, not the fits, so that this plot is model independent. The inset shows the temperature dependence of $1/\epsilon$ as determined from the peaks of the $\hat{H}_{c2}(\theta)/\hat{H}_{c2}(0^\circ)$ curves. The solid line in the inset is a fit to the functional form $1/\epsilon(t) = [1/\epsilon(0)](1+t)^{-1}$.

sample at three different reduced temperatures. As the figure shows, the curves for $t=0.76$ and 0.55 do indeed lie on top of one another, implying a nearly temperature-independent anisotropy in this temperature range. However, the curve for $t=0.29$ clearly lies above the other two curves near $\theta=90^\circ$, which suggests a small increase in $1/\epsilon$ at low temperatures. A similar plot of the $H_{c2}(\theta)$ data of Iye and Tanuma⁶ on C₈KHg shows that ϵ is also temperature dependent in the stage-2 KHg GIC.^{15,28} The temperature dependence of $1/\epsilon$ (as determined by the peaks of the curves in Fig. 8) is plotted in the inset to the figure. The solid line in the inset is a fit to the equation

$$1/\epsilon(t) = \frac{1/\epsilon(0)}{1+t}. \quad (7)$$

This functional form for $1/\epsilon(t)$ is implied by Eq. (2) if one assumes that $H_{c2,\perp\hat{c}}(T)$ depends linearly on T and $H_{c2,\parallel\hat{c}}(T)$ is quadratic in T . The reasonable agreement between the fit and the data in the inset to Fig. 8 demonstrates consistency between the $H_{c2}(T)$ fits and the $H_{c2}(\theta)$ data. Extension of the $H_{c2}(\theta)$ measurements to lower temperatures would provide a more rigorous test of this consistency.

The small low-temperature increase of ϵ is at least partially due to the quadratic temperature dependence of $\hat{H}_{c2,\parallel\hat{c}}$. A slight upturn in $H_{c2,\perp\hat{c}}$ at low temperatures could also cause an upturn in ϵ . Strong positive curvature of $H_{c2,\perp\hat{c}}$ has also been observed by Iye and Tanuma⁶ in second-stage C₈RbHg. However, there is no evidence for positive curvature of $H_{c2}(T)$ in KHg GIC's.

V. DISCUSSION

Several objections may be raised to the type-I superconductivity hypothesis. Firstly, the value of H_c obtained from the $H_{c2}(\theta)$ fit at $t=0.57$ in Fig. 4 (43 Oe) is considerably lower than the $H_c=75$ Oe that was predicted from specific-heat measurements at this reduced temperature. The ratio between the value of H_c calculated from the specific-heat measurements and the H_c obtained from the $H_{c2}(\theta)$ fits is about 1.8 for two $T_c=1.5$ K specimens at all three temperatures where $H_{c2}(\theta)$ measurements were performed. A second unexplained feature of the experimental data is that the $H_{c2}(\theta)$ curves are not perfectly flat near $\theta=0^\circ$, although H_c should be absolutely constant as a function of angle. Both of these discrepancies may be caused by angle-dependent demagnetization effects, which are hard to account for quantitatively.⁴⁰ Demagnetization effects can be large for platelike samples such as those used in these experiments.

In order to extract quantitative values for H_c from the $H_{c2}(\theta)$ fits, demagnetization corrections need to be applied. The angular dependence of the demagnetization factor of an oblate spheroidal superconductor has been worked out by Denhoff and Gyax.⁴⁰ However, the application of this formula to the C₄KHg data is not justified since it involves too many parameters that are either poorly known (e.g., the dimensions of the intercalated

sample) or not independently known (e.g., ϵ and the Ginzburg-Landau parameter κ). Therefore the demagnetization for the C₄KHg specimens has been estimated only for the high-symmetry directions by approximating the sample shape as ellipsoidal.

The samples used in the $H_{c2}(\theta)$ measurements were flat plates with typical dimensions on the order of $(2 \times 2 \times 0.5 \text{ mm}^3)$. Consultation of standard tables⁴¹ shows that a demagnetization correction of about 3 is anticipated for an ellipsoid with radii in the ratios 1:1:0.25 when the field is applied parallel to the shortest axis. If this correction is applied to the H_c values determined from the $H_{c2}(\theta)$ fits, one obtains $H_c(T=0) \approx 203$ Oe. This corrected H_c is now a factor of 1.8 *higher* than the $H_c(T=0)$ of 112 Oe calculated from the specific-heat data,³⁷ which were taken on low- T_c samples. Since $H_c \propto \sqrt{\gamma}$ and $\gamma \propto N(0)$, a higher H_c for the pink $T_c=1.5$ K specimens implies that they have a higher density of states $N(0)$ than the lower- T_c specimens used for the specific-heat studies. The higher $N(0)$ for the pink specimens is thus consistent with their higher value of T_c .

It is interesting to reexamine the fit to the data in Fig. 4, in which the arrow marks the corrected value of the thermodynamic critical field at $t=0.57$. The implication of this H_c estimate is that C₄KHg is type I in the approximate range $\theta < 80^\circ$ and type II for $\theta > 80^\circ$. Inclusion of demagnetization corrections therefore increases the angular range in which type-I behavior is expected for pink $T_c=1.5$ K C₄KHg specimens. In the type-I angular range, the form of $\hat{H}_{c2}(\theta)$ is completely determined by the angular-dependent demagnetization factor calculated by Denhoff and Gyax.⁴⁰ Magnetization measurements on C₄KHg are desirable to positively identify type-I superconductivity. Specific-heat measurements on $T_c=1.5$ K pink C₄KHg specimens would also be useful.

The extended linearity of $H_{c2}(T)$ reported here for $T_c=1.5$ K pink C₄KHg specimens is not surprising in light of previous studies of layered superconductors. Positive curvature or extended linearity of $H_{c2}(T)$ are phenomena common to almost all anisotropic superconducting compounds.¹¹ Depending on the specific type of the superconductor in question, many different explanations might be considered for the anomalous temperature dependence of H_{c2} . For example, mechanisms ranging from coupling-dimensionality crossover⁴² to proximity-effect-induced curvature⁴³ to magnetoresistive anomalies⁴⁴ have been cited as the cause of positive curvature in various superconductors. However, each of these explanations for its own reasons seems to be inappropriate for GIC's.²⁸ In order to choose an appropriate model from the many that are available, the best procedure is to consider what is already known about GIC's.

There are two types of models of anisotropic superconductivity that seem to contain the right features for the GIC superconductors: these are the anisotropic Fermi surface models^{45,46} and the multiband superconductivity models.^{47,48} Anisotropic Fermi-surface models are an obvious possibility because the quasi-two-dimensional band

structure of graphite is responsible for many of the characteristic properties of GIC's. The simplest anisotropy-based model available is that developed by Butler⁴⁵ to fit $H_{c2}(T)$ in Nb. This model was adapted by Dalrymple and Prober to fit their $H_{c2}(T)$ data for NbSe₂, which show extended linearity and positive curvature⁴⁹ similar to that seen in GIC's. The NbSe₂ Fermi surface has cylindrical pieces at the hexagonal Brillouin-zone boundary, and bears a great deal of resemblance to the proposed Fermi surface of many of the GIC's.^{50,51} The band structure of C₄KHg has been calculated,⁵² but unfortunately not enough quantitative information about the Fermi surface has been reported to allow a detailed comparison between the Butler model and the $H_{c2}(T)$ data for C₄KHg.

Another well-established feature of the GIC's Fermi surface is the presence of multiple bands. Some of the bands at the Fermi surface of graphitic origin are nearly two dimensional in character. Other bands, which may be either of intercalant or graphitic origin, are more three dimensional (3D) in character. In C₄KHg these 3D bands are derived from hybridized K and Hg levels.⁵² Models for $H_{c2}(T)$ that incorporate the participation of two types of bands in the superconductivity therefore appear to be a logical choice for GIC's. Entel and Peter⁴⁷ have fit $H_{c2}(T)$ data for Cs_{0.1}WO_{2.9}F_{0.1}, a tungsten fluoroxide bronze, using a two-band Fermi-surface model. Al-Jishi⁵³ has proposed a similar model specifically tailored to fit critical-field data on C₈K, although calculations using this model are still preliminary.

The idea that both graphitic and intercalant bands participate in GIC superconductivity is sensible for two reasons. One reason is that there are superconducting GIC's [specifically the binary compounds C₈K (Ref. 4) and C₈Rb (Ref. 54)] that are synthesized from nonsuperconducting starting materials. Since the KHg GIC's are synthesized from KHg amalgams, which are themselves superconducting, it might be thought that this argument for multiband superconductivity does not apply to them. However, the increase of T_c with stage index in the KHg GIC's is contrary to expectations of the superconducting proximity effect^{55,56} if the carbon layers are not also participating in the superconductivity. The large critical-field anisotropy seen in GIC's is also difficult to explain if graphitic electrons are not involved.^{48,57}

It is reasonable to expect a common origin for the extended linearity of $H_{c2}(T)$ and the deviations of the experimental points from Eq. (1) in the $H_{c2}(\theta)$ fits. However, the deviations of the $H_{c2}(T)$ data from the WHH theory occur at the lowest obtainable reduced temperatures. The $H_{c2}(\theta)$ fits to Eq. (1), on the other hand, worsen as the temperature is increased toward T_c .²⁸ Poorer agreement between Eq. (1) and the data as temperature is increased is expected if type-I superconductivity is the origin of the discrepancy. This trend has already been observed for TaN.³⁸ All the available evidence therefore points to type-I superconductivity as the explanation of the poor quality of the fits shown in Fig. 3.

It was not necessary to make allowance for type-I char-

acter to fit the $H_{c2}(\theta)$ curves of the gold, mixed-phase samples, a finding that is consistent with the observations of Iye and Tanuma.⁶ Type-II character for all orientations of lower- T_c C₄KHg is due to the fact that the $T_c=0.8$ K samples have critical fields almost as high as the $T_c=1.5$ K samples. To be more specific, the typical extrapolated value of $H_{c2,\perp\hat{c}}(T=0)$ for a $T_c=1.5$ K C₄KHg specimen is only about 750 Oe, while that for the $T_c=0.8$ K specimens is about 650 Oe.⁶ The critical-field slope at T_c in the WHH model is $dH_{c2}/dT = 4k_B/\pi eD$, where k_B and e are the usual fundamental constants and $D = v_F l/3$ is the diffusivity.^{10,39} Therefore the higher dH_{c2}/dT in the mixed-phase samples suggests that they have either a lower mean-free path l or a smaller Fermi velocity v_F . The greater in-plane disorder of the mixed-phase samples would appear to favor the lower mean-free-path explanation.

VI. HYDROGENATION AND PRESSURE EXPERIMENTS

The remaining unsettled issue for C₄KHg is the question of the difference between the pink and gold types of C₄KHg. The experimentally verified differences between the two types of specimens are summarized in Table II. As mentioned previously, extensive characterization of the specimens used for the low-temperature measurements²⁸ suggests that the only normal-state difference between the gold, lower- T_c samples and the pink, $T_c=1.5$ K samples is that the gold specimens contain both the α and β phases, while the pink specimens contain only the α phase. While this finding is of great interest, it is far from an explanation of the T_c difference between the pink and gold samples. The suppression of the bulk T_c of a superconductor by the presence of a small amount of a second phase is unusual if the second phase is not ferromagnetic. Certainly no magnetic ordering is anticipated in the β phase of C₄KHg.

Previously reported experiments on the hydrogenation¹³ and application of pressure⁵⁹ to C₄KHg may help to clarify the question of the two types of C₄KHg. The hydrogenation experiments¹³ showed that a minute amount of hydrogen gas can increase the T_c of the gold mixed-phase specimens to 1.5 K, and dramatically narrow the superconducting transition.¹³ The results of the applied pressure experiments were strikingly similar:⁵⁹ a small hydrostatic pressure of 0.8 kbar narrows an initially very broad superconducting transition and increases T_c . The most obvious explanation for the hydrogenation and pressure results would seem to be that application of pressure or exposure to hydrogen converts the minority β phase to the majority α phase, raising T_c . However, this hypothesis is not supported by neutron diffraction experiments performed by Kim *et al.*,²¹ which show that the fraction of α and β phases in a mixed-phase sample is not changed by pressures up to 13.8 kbar.

DeLong and Eklund proposed two ideas to explain the $T_c(P)$ data.⁵⁹ One proposal is that the pressure induces

a disorder-order structural phase transformation that increases T_c and narrows the superconducting transition. A problem with this hypothesis has been pointed out by Clarke and Uher,¹ who note that the reversibility of the pressure-induced transformation at $T \approx 1$ K is inconsistent with a disorder-order transformation.

The second mechanism proposed by DeLong and Ekland to explain the effect of applied pressure on T_c involves suppression of a charge-density-wave (CDW) state.⁵⁹ A small amount of applied pressure has been observed to sharply increase T_c in many transition-metal dichalcogenide (TMDC) superconductors.⁶⁰ Those TMDC's have a coexisting CDW state and superconducting order at low temperature. The application of pressure increases T_c by suppressing the CDW state.⁶¹ In some TMDC superconductors, T_c can also be increased by low-level hydrogenation.⁶²

An explanation of the effect of applied pressure and hydrogenation on the two phases of $C_4K\text{Hg}$ can be worked out by analogy to the TMDC CDW-suppression model. In this picture, only the higher I_c β phase of $C_4K\text{Hg}$ undergoes a CDW distortion at some $T > T_c$. This CDW transition removes a portion of the $C_4K\text{Hg}$ Fermi surface, which reduces the density of states at the Fermi level, $N(0)$. The reduced $N(0)$ in the β phase at low temperature decreases the T_c of mixed ($\alpha + \beta$) samples to about 0.8 K. Hydrogenation or application of pres-

sure can then suppress the CDW and restore $N(0)$ to its high-temperature value, thereby increasing T_c of the ($\alpha + \beta$) phase samples to the 1.5 K seen in pure α -phase specimens.

Iye⁸ has studied the effect of high pressure on the transition temperature of the pure α -phase ($T_c = 1.5$ K at atmospheric pressure) $C_4K\text{Hg}$ samples and found that hydrostatic pressure lowers T_c in these samples. This result is completely consistent with the existence of a CDW state in the lower- T_c ($\alpha + \beta$) phase samples. In the case of the TMDC superconductors, the application of pressure beyond that necessary to suppress the CDW may either decrease or further increase T_c .⁶⁰

Though none of these similarities between the TMDC's and $C_4K\text{Hg}$ is direct evidence for the presence of a CDW, the possibility of a CDW instability has previously been mentioned in connection with band-structure calculations for C_8K .⁵⁰ The periodic lattice distortion that is associated with CDW formation has never been observed in x-ray^{18,20} or neutron-diffraction¹⁹ experiments on $C_4K\text{Hg}$. This is not proof of the nonexistence of a CDW, since usually the periodic lattice distortion is easily observed only in electron diffraction⁶¹ or scanning tunneling microscopy experiments.⁶³ In light of the evidence that suggests the presence of a CDW in $C_4K\text{Hg}$, temperature-dependent microscopy studies of $C_4K\text{Hg}$ would be highly desirable. A search for resis-

TABLE II. A summary of the known differences between the pink and gold $C_4K\text{Hg}$ samples. The numbers here are for a typical sample of a given type, although some variation is observed from sample to sample. The reasons for the discrepancy between the values of $1/\epsilon$ determined from dH_{c2}/dT and $\hat{H}_{c2}(\theta)$ are discussed in the text. ξ is the superconducting coherence length (Ref. 33).

Property	Expt.	Pink	Gold
Primary I_c	diffraction ^{a,b}	10.24 Å	10.24 Å
Secondary I_c	diffraction ^{a,b}	NA ^c	10.83 Å
Primary structure	neutrons ^a ;TEM ^d	(2 × 2)R0°	(2 × 2)R0°
Secondary structure	neutrons ^a ;TEM ^d	NA ^c	(√3 × 2)R(30°, 0°)
Stoichiometry	chemical analysis	$C_{4.3}K\text{Hg}_{1.1}$	$C_{4.7}K\text{Hg}_{1.2}$
T_c	inductive	1.5 K	0.8 K
T_c (hydrogenated)	inductive	1.5 K ^e	1.5 K ^e
$\xi_{\parallel\hat{c}}(T = 0)$	$H_{c2}(T = 0)$	225 Å	200 Å
$\xi_{\perp\hat{c}}(T = 0)$	$H_{c2}(T = 0)$	2000 Å	2400 Å
Types I and II ^f $\parallel \hat{c}$	$H_{c2}(T)$, C_F ^g	NA ^c	Type II
Types I and II ^f $\perp \hat{c}$	$H_{c2}(T)$, C_F ^g	NA ^c	Type II
Types I and II ^f $\parallel \hat{c}$	$H_{c2}(T)$, $\hat{H}_{c2}(\theta)$	Type I	NA ^c
Types I and II ^f $\perp \hat{c}$	$H_{c2}(T)$, $\hat{H}_{c2}(\theta)$	Type II	NA ^c
$dH_{c2,\perp\hat{c}}/dT _{T_c}$	$H_{c2}(T)$	500 Oe/K	800 Oe/K
$dH_{c2,\parallel\hat{c}}/dT _{T_c}$	$H_{c2}(T)$	60 Oe/K	75 Oe/K
$1/\epsilon$	dH_{c2}/dT	8	11
$1/\epsilon$	$\hat{H}_{c2}(\theta)$	7-10	11

^aReference 19.

^bReference 23.

^cNA means not applicable.

^dReference 58.

^eReference 13.

^fPiecewise continuous function given by Eq. (5).

^gReference 37.

tivity and susceptibility anomalies associated with CDW formation in $T_c=0.8$ K samples would also be of interest.

VII. CONCLUSIONS

The GIC superconductors display a number of anomalous superconducting properties, many of which can be understood in terms of the participation of graphitic electrons in superconductivity. Among the unusual properties that the class of GIC superconductors exhibits are large critical-field anisotropy $1/\epsilon$, extended linearity or positive curvature of the critical fields $H_{c2}(T)$, and both type-I and type-II superconductivity in the same specimen for different applied field orientations.

These features have been studied in C_4KHg , the first stage KHg GIC, with a particular emphasis on understanding the reason for the two different superconducting transition temperatures reported in this compound. The lower T_c of 0.8 K found in gold-colored specimens is associated with the presence of the $I_c=10.83$ Å β phase. Superconducting properties are reported for the pink single-phase specimens, which have only a single repeat distance, $I_c=10.24$ Å. The $T_c=1.5$ K single-phase samples are similar to the mixed-phase specimens except that the pink samples have slightly lower critical-field slopes dH_{c2}/dT , resulting in type-I behavior for applied field orientations near $\mathbf{H} \parallel \hat{c}$. $H_{c2}(t)$ has been measured for a large reduced temperature range for the $T_c=1.5$ K

C_4KHg samples, and an approximately linear temperature dependence has been found for $\mathbf{H} \perp \hat{c}$. This extended linearity is reminiscent of that seen in $NbSe_2$ and other TMDC's.⁴⁹ Competition between superconductivity and a charge-density wave is another common feature of the TMDC's.⁶⁰ The presence of a CDW instability in the β phase of C_4KHg may help to explain the effect of hydrogen¹³ and applied pressure⁵⁹ on the T_c for this compound. The proposed CDW has yet to be directly observed experimentally.

ACKNOWLEDGMENTS

The authors would like to thank Eric Tkaczyk and J.A.X. Alexander for providing an algorithm on which the critical-field fitting routine was based. We would also like to thank Eliot Dresselhaus for installing the software that produced the figures in this paper. We would like to thank G. Doll, J. Speck, Y. Iye, T. Enoki, and R. Al-Jishi for their advice on this project. The authors A.C., M.S.D., and G.D. gratefully acknowledge support by U.S. Air Force of Scientific Research (AFOSR) Contract No. F49620-83-C-0011 for the early stages of this work and National Science Foundation (NSF) Grant No. DMR 83-10482 for support during the past year. The Francis Bitter National Magnet Laboratory is supported by the NSF.

*Present address: Naval Research Lab., Code 6345, 4555 Overlook Ave. SW, Washington, D.C. 20375.

¹Present address: NSF, Division of Materials Research, 1800 G St. NW, Washington, D.C. 20550.

²R. Clarke and C. Uher, *Adv. Phys.* **33**, 469 (1984).

³*Intercalation in Layered Materials*, edited by M. S. Dresselhaus (Plenum, New York, 1987).

⁴N. B. Hannay, T. H. Geballe, B. T. Matthias, K. Andres, P. Schmidt, and D. MacNair, *Phys. Rev. Lett.* **14**, 255 (1965).

⁵Y. Koike, H. Suematsu, K. Higuchi, and S. Tanuma, *J. Phys. Chem. Solids* **41**, 1111 (1980).

⁶S. A. Solin and H. Zabel, *Adv. Phys.* **37**, 87 (1988).

⁷Y. Iye and S. Tanuma, *Phys. Rev. B* **25**, 4583 (1982).

⁸L. A. Pendry, R. Wachnik, F. L. Vogel, P. Lagrange, G. Furdin, M. El Makrini, and A. Hérold, *Solid State Commun.* **38**, 677 (1981).

⁹Y. Iye, in *Proceedings of the Symposium on Intercalated Graphite, Boston, 1982*, edited by M. S. Dresselhaus, G. Dresselhaus, J. E. Fischer, and M. J. Moran, (North-Holland, New York, 1983), Vol. 20, p. 185.

¹⁰E. Helfand and N. R. Werthamer, *Phys. Rev.* **147**, 288 (1966).

¹¹T. P. Orlando, E. J. McNiff, Jr., S. Foner, and M. R. Beasley, *Phys. Rev. B* **19**, 4545 (1979).

¹²J. A. Woollam, R. B. Somoano, and P. O'Connor, *Phys. Rev. Lett.* **32**, 712 (1974).

¹³G. Timp, B. S. Elman, R. Al-Jishi, and G. Dresselhaus,

Solid State Commun. **44**, 987 (1982).

¹⁴G. Roth, A. Chaiken, T. Enoki, N. C. Yeh, G. Dresselhaus, and P. M. Tedrow, *Phys. Rev. B* **32**, 533 (1985).

¹⁵G. Timp and M. S. Dresselhaus, *J. Phys. C* **17**, 2641 (1984).

¹⁶A. Chaiken, T. P. Orlando, P. M. Tedrow, and G. Dresselhaus, in *Multilayers: Synthesis, Properties, and Non-electronic Applications*, edited by T. W. Barbee, Jr., F. Spaepen, and L. Greer (Materials Research Society, Pittsburgh, 1988), Vol. 103.

¹⁷M. El Makrini, P. Lagrange, and A. Hérold, *Carbon* **18**, 374 (1980).

¹⁸M. El Makrini, G. Furdin, P. Lagrange, J. F. Mareche, E. McRae, and A. Hérold, *Synth. Met.* **2**, 197 (1980).

¹⁹M. El Makrini, Ph.D. thesis, Université de Nancy, 1980.

²⁰W. A. Kamitakahara, L. E. DeLong, P. C. Eklund, and R. M. Nicklow, *Phys. Rev. B* **29**, 460 (1984).

²¹M. El Makrini, D. Guérard, P. Lagrange, and A. Hérold, *Physica* **99B**, 481 (1980).

²²H. J. Kim, H. Mertwoy, T. Koch, J. E. Fischer, D. B. McWhan, and J. D. Axe, *Phys. Rev. B* **29**, 5947 (1984).

²³G. Timp, T. C. Chieu, P. D. Dresselhaus, and G. Dresselhaus, *Phys. Rev. B* **29**, 6940 (1984).

²⁴P. Lagrange, M. El Makrini, and A. Bendriss, *Synth. Met.* **7**, 33 (1983).

²⁵P. Lagrange, M. El Makrini, and A. Hérold, *Rev. Chim. Miner.* **20**, 1983 (1983).

²⁶P. R. Bevington, *Data Reduction and Error Analysis for*

- the Physical Sciences* (McGraw-Hill, New York, 1969).
- ²⁶W. C. Hamilton, *Acta Crystallogr.* **18**, 502 (1965).
- ²⁷J. D. Axe and J. B. Hastings, *Acta Crystallogr. Sect. A* **39**, 593 (1983).
- ²⁸A. Chaiken, Ph.D. thesis, Massachusetts Institute of Technology, 1988.
- ²⁹M. H. Yang, P. C. Eklund, and W. A. Kamitakahara, in *Extended Abstracts of the Symposium on Intercalated Graphite at the Materials Research Society Meeting, Boston, 1984*, edited by M. S. Dresselhaus, G. Dresselhaus, and S. Solin (Materials Research Society, Pittsburgh, 1988), p. 125.
- ³⁰W. A. Kamitakahara, P. C. Eklund, L. E. DeLong, and M. H. Yang, in *Proceedings of the 17th International Conference on Low-Temperature Physics, Karlsruhe, 1984*, edited by U. Eckern, A. Schmid, W. Weber, and W. Wuehl (North-Holland, Amsterdam, 1984), p. 861.
- ³¹G. Roth, N. Yeh, A. Chaiken, G. Dresselhaus, and P. Tedrow, in *Extended Abstracts of the Symposium on Intercalated Graphite at the Materials Research Society Meeting, Boston, 1984*, Ref. 29, p. 149.
- ³²W. R. Abel, A. C. Anderson, and J. C. Wheatley, *Rev. Sci. Instrum.* **35**, 444 (1964).
- ³³M. Tinkham, *Introduction to Superconductivity* (Krieger, Huntington, New York, 1980).
- ³⁴S. Tanuma, Y. Iye, and Y. Koike, *Physics of Intercalation Compounds*, Vol. 38 of *Springer Series in Solid-State Physics* (Springer-Verlag, Berlin, 1981), p. 298.
- ³⁵R. C. Morris, R. V. Coleman, and R. Bhandari, *Phys. Rev. B* **5**, 895 (1972).
- ³⁶E. I. Kats, *Zh. Eksp. Teor. Fiz.* **56**, 1675 (1969) [*Sov. Phys.—JETP* **29**, 897 (1969)].
- ³⁷M. G. Alexander, D. P. Goshorn, D. Guérard, P. Lagrange, M. El Makrini, and D. G. Onn, *Solid State Commun.* **38**, 103 (1981).
- ³⁸H. W. Weber, J. F. Sporna, and E. Seidl, *Phys. Rev. Lett.* **41**, 1502 (1978).
- ³⁹D. Saint-James, G. Sarma, and E. J. Thomas, *Type II Superconductivity* (Pergamon, New York, 1969).
- ⁴⁰M. W. Denhoff and S. Gyax, *Phys. Rev. B* **25**, 4479 (1982).
- ⁴¹J. A. Osborn, *Phys. Rev.* **67**, 351 (1945).
- ⁴²R. A. Klemm, A. Luther, and M. R. Beasley, *Phys. Rev. B* **12**, 877 (1975).
- ⁴³K. R. Biagi, V. G. Kogan, and J. R. Clem, *Phys. Rev. B* **32**, 7165 (1985).
- ⁴⁴L. E. DeLong, G. W. Crabtree, L. N. Hall, D. G. Hinks, W. E. Kwok, and S. K. Malik, *Phys. Rev. B* **36**, 7155 (1987).
- ⁴⁵W. H. Butler, *Phys. Rev. Lett.* **44**, 1516 (1980).
- ⁴⁶D. W. Youngner and R. A. Klemm, *Phys. Rev. B* **21**, 3890 (1980).
- ⁴⁷P. Entel and M. Peter, *J. Low Temp. Phys.* **22**, 613 (1976).
- ⁴⁸R. Al-Jishi, *Phys. Rev. B* **28**, 112 (1983).
- ⁴⁹B. J. Dalrymple and D. E. Prober, *J. Low Temp. Phys.* **56**, 545 (1984).
- ⁵⁰T. Inoshita, K. Nakao, and H. Kamimura, *J. Phys. Soc. Jpn.* **43**, 1237 (1977).
- ⁵¹D. P. DiVincenzo and S. Rabi, *Phys. Rev. B* **25**, 4110 (1982).
- ⁵²N. A. W. Holzwarth and S. D. Had, *Phys. Rev. B* **38**, 3722 (1988).
- ⁵³R. Al-Jishi, A. Chaiken, and M. S. Dresselhaus, in *Extended Abstracts of the Symposium on Graphite Intercalation Compounds at the Materials Research Society Meeting, Boston, 1988*, edited by M. Endo, M. S. Dresselhaus, and G. Dresselhaus (Materials Research Society, Pittsburgh, 1988), p. 53.
- ⁵⁴M. Kobayashi, T. Enoki, H. Inokuchi, M. Sano, A. Sumiyama, Y. Oda, and H. Nagano, *J. Phys. Soc. Jpn.* **54**, 2359 (1985).
- ⁵⁵N. R. Werthamer, *Phys. Rev.* **132**, 2440 (1963).
- ⁵⁶P. G. deGennes, *Superconductivity of Metals and Alloys* (Benjamin, New York, 1966).
- ⁵⁷Y. Takada, *J. Phys. Soc. Jpn.* **51**, 63 (1982).
- ⁵⁸G. Timp, B. S. Elman, M. S. Dresselhaus, and P. Tedrow, in *Proceedings of the Symposium on Intercalated Graphite, Boston, 1982*, edited by M. S. Dresselhaus, G. Dresselhaus, J. E. Fischer, and M. J. Moran (North-Holland, New York, 1983), Vol. 20.
- ⁵⁹L. E. DeLong and P. C. Eklund, *Synth. Met.* **5**, 291 (1983).
- ⁶⁰R. H. Friend and D. Jérôme, *J. Phys. C* **12**, 1441 (1979).
- ⁶¹J. A. Wilson, F. J. DiSalvo, and S. Mahajan, *Adv. Phys.* **24**, 117 (1975).
- ⁶²D. W. Murphy, F. J. DiSalvo, G. W. Hull, Jr., J. V. Wasczak, S. F. Meyer, G. R. Stewart, S. Early, J. V. Acrivos, and T. H. Geballe, *J. Chem. Phys.* **62**, 967 (1975).
- ⁶³R. V. Coleman, B. Drake, P. K. Hansma, and G. Slough, *Phys. Rev. Lett.* **55**, 394 (1985).